Microporous and Mesoporous Materials 372 (2024) 113097

Contents lists available at ScienceDirect

Microporous and Mesoporous Materials

journal homepage: www.elsevier.com/locate/micromeso

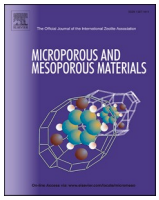

Catalytic potential of green ordered mesoporous carbons, obtained from biomass-derived xylose, glucose, and lignin

Anna Casadó [a], Anies Rösch [a], Angie C. Rueda [a], Alejandro Uribe [a], M. Dolores González [a], Aroldo J. Romero [b], Joan J. Carvajal [a], Yolanda Cesteros [a,*]

[a] Universitat Rovira i Vigili, Departament de Química Física i Inorgànica, C/ Marcel·lí Domingo, 1, 43007, Tarragona, Spain
[b] Eurecat, Centre Tecnològic de Catalunya, C/ Marcel·lí Domingo, 43007, Tarragona, Spain

ARTICLE INFO

Keywords:
Ordered mesoporous carbons
Xylose
Glucose
Lignin
Heterogeneous catalysts

ABSTRACT

Green high-surface area Ordered Mesoporous Carbons (OMCs) (576–948 m^2/g) were successfully synthesized by the hard template method using xylose, glucose and lignin solutions obtained from almond shells, a local biomass waste, as carbon precursors, and SBA-15 as a template. The catalytic potential of OMCs, as catalytic supports or as catalysts, has been preliminarily tested for different reactions of interest. A dried sulfonic-acid treated OMC, obtained from xylose extract, led to full conversion and 92% selectivity to di- and tri-ethers of glycerol for the glycerol etherification with isobutene at 80 °C. A sulfonic-acid treated OMC, obtained from glucose, presented a higher turnover frequency (TOF) value and slightly lower selectivity to levulinic acid than commercial Amberlyst-15 for the conversion of 5-hydroxymethylfurfural at 180 °C. The use of an OMC obtained from lignin as catalytic support of a nickel catalyst combined with H-Beta led to 78% of selectivity to cyclohexane at total conversion for the hydrodeoxygenation of guaiacol at 180 °C.

1. Introduction

The development of technologies to produce energy and chemical products from renewable resources, as an alternative to petroleum products, has promoted the valorization of biomass. Lignocellulose, the most abundant renewable biomass, contains three polymers: cellulose (40–50%), hemicellulose (25–35%) and lignin (15–20%). Glucose and xylose can be obtained from cellulose and hemicellulose, respectively.

One interesting way for valorizing lignocellulosic biomass wastes is the synthesis of carbons with controlled pore size using templates, the so-called Ordered Mesoporous Carbons (OMC) [1,2]. These materials are potential catalytic supports or, after acid-functionalization, catalysts due to their non-toxicity, degradability, and high surface area.

There are two main methodologies for preparing OMCs: soft and hard templating. The soft template method requires the use of block copolymers, surfactants, or organic compounds as templates, which are confined with low interaction in the prepared framework. The hard template method consists of using an inorganic solid as a template filling its porous network with a carbon precursor solution followed by carbonization. The template is removed at the end of the synthesis, in both methods, to obtain the ordered pore system [2].

Ordered mesoporous silicas have become the most used hard templates due to their ordered structure, high stability, and reproducibility [3–7] with special mention to SBA-15, widely applied due to its interconnections between the mesoporous channels that favor the formation of the replica structure [6,7]. The filling of the silica pores is the most critical stage for the replication success. The carbon precursor must have suitable dimensions and favorable interactions with the silica walls. Commercial sucrose, furfuryl alcohol, phenol resin, and acetonitrile propylene, among others have been used as carbon precursors for the hard templating method [8]. However, there are few references about the use of carbon precursors obtained from biomass wastes, only some finger citron residues, wheat starch or Arabic gum [8]. The use of lignocellulosic biomass, as a raw material, for synthesizing OMCs instead of commercial carbon precursors, is an interesting way to add value to these wastes, thus making a significant contribution to the principles of circular bioeconomy. There are also few references about the use of OMCs in catalysis [9–13].

Catalytic etherification of glycerol with t-butanol or isobutene to obtain biofuel additives, di- and triethers of glycerol (h-GTBE), is an acid-catalyzed reaction of interest to revalorize glycerol, a surplus obtained in high amounts during biodiesel production (Scheme 1a).

* Corresponding author. Dpt. Química Física i Inorgànica, Universitat Rovira i Virgili, C/Marcel·lí Domingo s/n, 43007, Tarragona, Spain.
E-mail address: yolanda.cesteros@urv.cat (Y. Cesteros).

https://doi.org/10.1016/j.micromeso.2024.113097
Received 27 November 2023; Received in revised form 13 March 2024; Accepted 19 March 2024
Available online 20 March 2024

Sulfonic acid-functionalized materials, such as ordered mesoporous silicas, zeolites, clays or aerogels have been tested for this reaction [14–17]. Sulfonated SBA-15 and sulfonated beta zeolite achieved total conversion and high selectivity (up to 91 %) towards h-GTBE at 75 °C [14]. The amount and strength of Brønsted acid sites affected conversion, the acidity strength influenced the formation of h-GTBE, and the accessibility of the reagents to the acid sites required an optimal reaction time for each material [15]. There are a few references of using carbons in this reaction [18–20]. Frusteri et al. achieved 89.9 % yield to h-GTBE using carbon microspheres treated with HNO_3 at 70 °C after 6 h of reaction [19].

5-Hdroxymethylfurfural (5-HMF) is one of the most versatile platform molecules, obtained from lignocellulosic biomass, since it can be transformed into high-added value products such as levulinic acid (LeA), a bioplastic precursor, through an acid-catalyzed reaction (Scheme 1b). Montmorillonite, sulfonated solids, heteropolyacids, biochars and zeolites have been used as acid catalysts for the obtention of LeA from glucose, fructose or cellulose [21–23]. However, there are very few references about its obtention from 5-HMF. Song et al. obtained 74.1 % conversion and 82.2 % selectivity to LeA at 140 °C after 2 h from 5-HMF in water using a Brønsted acidic ionic liquid functionalized mesoporous organosilica nanospheres catalyst [24]. The formation of by-products, such as humins, due to the oligo-, polymerization of 5-HMF, or by esterification of 5-HMF with LeA, can deactivate the catalyst.

Another interesting reaction to reduce the significant dependence on petroleum-derived transportation fuels is the hydrodeoxygenation (HDO) of lignin to produce hydrocarbons. This process involves decarbonylation, decarboxylation, deoxygenation, hydrogenolysis, hydrocracking and hydrogenation reactions. For this reason, this reaction is mainly studied using lignin model compounds, such as guaiacol [25–27]. M. López et al. tested an ordered mesoporous carbon, obtained from furfuryl alcohol, as support for dispersing Ni–ZrO_2 active phases for HDO of guaiacol obtaining high conversion and high selectivity towards the hydrogenation product (methoxycyclohexanol) and the hydrogenated-deoxygenated products (cyclohexanol and cyclohexane) at 300 °C and 50 bars of H_2 [27]. Interestingly, X. Wang et al. studied the hydrodeoxygenation of guaiacol to cyclohexane at lower temperatures (140 °C) over Ni/SiO_2 catalyst combined with H-β zeolite [26]. This catalyst resulted in a 91.7% yield of cyclohexane. The main reaction products obtained at reaction temperatures below 200 °C are indicated in Scheme 1c.

The main objective of this work is the preparation of green ordered mesoporous carbons (OMCs) by the hard template method, using different fractions of biomass (glucose, xylose and lignin) obtained from almond shells of the Tarragona region, as carbon precursors, and a mesoporous silica (SBA-15) as a template. This approach aims to add value to the whole lignocellulosic biomass waste, contributing to the development of the circular bioeconomy. Different parameters, such as the carbon precursor/template ratio, the use of ultrasound during impregnation of the template, the addition of acid medium, the carbonization temperature or the extract concentration were optimized for each biomass fraction. Additionally, to show the catalytic potential of these biobased materials, they have been preliminarily tested as catalysts or as catalytic supports for three reactions of interest: catalytic etherification of glycerol to di + triethers of glycerol (biofuel additives), catalytic conversion of 5-hydroxymethylfurfural to levulinic acid (bioplastic precursor), and catalytic hydrodeoxygenation of guaiacol to obtain biofuel components.

2. Experimental

2.1. Preparation of biomass extract solutions from almond shells

Almond shells were supplied by Cooperativa Unió Nuts (Reus). Xylose extract solutions were obtained from almond shells following the procedure described elsewhere [28]. 5 g of grounded almond shells were mixed in 50 mL of 1% (m/v) H_2SO_4 solution in a sealed Teflon reactor and heated at 120 °C for 1 h with microwaves under magnetic stirring. The microwave equipment used was a Milestone Ethos Touch control laboratory apparatus working at a frequency of 2.45 GHz and equipped

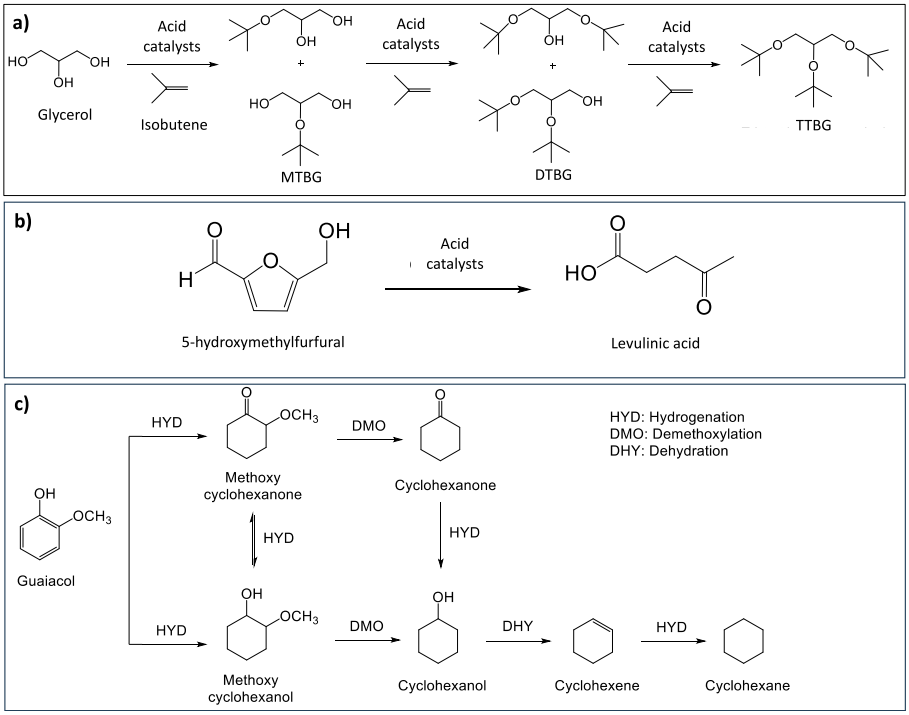

Scheme 1. a) Catalytic etherification of glycerol with isobutene to obtain h-GTBE: glycerol diethers + glycerol triether. MTBG: mono-*tert*-butyl glycerol ethers; DTBG: di-*tert*-butyl glycerol ethers; TTBG: tri-*tert*-butyl glycerol ethers; b) Catalytic dehydration of 5-hydroxymethylfurfural to levulinic acid; c) Catalytic hydrodeoxygenation of guaiacol at low reaction temperatures.

with a temperature controller. The irradiation microwave was programmed to work at a maximum of 400 W. The solid obtained was filtered and the liquid phase was stored as "xylose extract" in the fridge. The concentration of xylose in the extract solution was 12 g/L, as determined by HPLC chromatography with a RI detector using a RezexRHM-Monosaccharide H+(8%) column. The solid residue (R1) was washed with distilled water until pH > 5 and dried at 40 °C.

The Organosolv method was used for extracting lignin. 2.6 g of the dry solid R1 were mixed with 50 mL of a 3:1 (v/v) ethanol:water solution overnight at room temperature. Then, the mixture was heated with microwaves (400 W) in an autoclave under stirring at 180 °C for 20 min. The resulting liquid containing the solubilized lignin extract 1, was filtered off. The solid residue (R2) was washed with distilled water and dried at 40 °C. A lignin extract 2 was prepared following the same procedure as obtaining lignin extract 1 but starting from 7.8 g of dry solid R1. The concentrations of lignin extract 1 and lignin extract 2 were determined as 21 g/L and 49.5 g/L, respectively, by weighting the solid obtained by evaporation at 40 °C considering the known efficient separation and high-purity of the lignin obtained by the Organosolv method [29].

Finally, to obtain the glucose extract, 2 g of dry solid R2 was mixed with 50 mL of a 0.4 % (m/v) H_2SO_4 solution in a stainless-steel stirred autoclave and heated at 220 °C for 15 min by conventional heating, following the method reported elsewhere [30]. The resulting liquid was filtered off and stored as "glucose extract" in the fridge. The concentration of glucose in the extract was 26 g/L, as quantified by using a fructose/glucose assay kit (Cygic Biocon SL) and measuring the absorbance of glucose at 340 nm with a UV-VIS VWR 3100 PC spectrophotometer equipment.

2.2. Preparation of ordered mesoporous carbons

Samples were prepared by impregnation of ordered mesoporous silica SBA-15, which was used as a template, with glucose, xylose or lignin solutions, obtained from almond shells, and with commercial D-(+)-glucose (≥99%, BDH Prolabo) and D-(+)-xylose (≥99%, Merck) for comparison. Different carbon precursor/SBA-15 wt ratios were required to obtain the ordered mesoporous structures depending on the biomass fraction used. Here, the optimized results are shown.

2.2.1. Preparation of SBA-15

SBA-15 was prepared by adding 4.0 g triblock copolymer poly (ethylene glycol)-block-poly (propylene glycol)-block-poly (ethylene glycol) (EO20PO20EO20) (Merck) to a solution of 25 g HCl (37 wt %, Thermo Fisher Scientific) and 125 g of water under stirring for 2 h. Then, 8.6 g TEOS (98 %, Acros Organics Chemicals) was added, and the mixture was stirred at 40 °C for 20 h. Finally, this was transferred to a Teflon-lined autoclave and heated at 100 °C for 24 h. The resulting solid was filtered, washed repeatedly with distilled water, air dried at room temperature, and calcined in air at 500 °C for 6 h to remove the surfactant.

2.2.2. Preparation of ordered mesoporous carbons from xylose

Commercial xylose and SBA-15 were physically mixed in a weight ratio of 6:1, carbonized in a quartz reactor with a nitrogen flow of 100 mL/min at 650 °C for 2 h, and ground to obtain a homogenous powder. The elimination of the SBA-15 template was performed by refluxing the carbonized material with 100 mL of 0.625 M NaOH at 90 °C for 24 h. The resulting solid was filtered, washed with distilled water, and dried (sample *C*-Xyl-C1).

Another sample from commercial xylose was prepared by impregnation (sample *C*-Xyl-C2). First, 6 g of commercial xylose was dissolved in 5 mL of distilled water. Then, 0.2 g of concentrated sulfuric acid (98 wt %, Scharlau) and 1 g of SBA-15 were added and stirred for 10 min with ultrasound (Selecta H3000838). The mixture was rota-evaporated under vacuum at 50 °C. The sample was completely dried in an oven. Carbonization, elimination of the SBA-15 template, and later washing-drying steps were made at the same conditions as those used for obtaining *C*-Xyl-C1.

Three carbons were prepared using the xylose extract obtained from almond shells (*C*-Xyl-E1, *C*-Xyl-E2 and *C*-Xyl-E3). Sulfuric acid was not added since the xylose extract was already acid due to the 1 % H_2SO_4 aqueous medium used to obtain it. Ultrasound were applied in some steps to favor the diffusion of the xylose into the pores of the SBA-15.

For preparing sample *C*-Xyl-E1, the appropriate amount of xylose extract solution was evaporated in an oven at 60 °C until observation of a gelatinous aspect of the extract (2 days). Then, the sample was mixed with 1 g of SBA-15 applying ultrasound for 10 min. In order to promote xylose polymerization, the mixture was heated in a muffle at 100 °C for 6 h and at 160 °C for 6 h, following a method previously reported for sucrose [3]. Carbonization, elimination of the SBA-15 and later washing-drying steps were performed at the same conditions as those used to obtain the carbons from commercial xylose.

Sample *C*-Xyl-E2 was prepared by impregnation. The appropriate amount of xylose extract was mixed with 1 g of SBA-15 and stirred under ultrasound for 10 min. The mixture was rota-evaporated under vacuum at 50 °C. The sample was dried in an oven. Carbonization, elimination of the SBA-15 and later washing-drying steps were carried out at the same conditions as those used for obtaining the other carbons from xylose.

Finally, sample *C*-Xyl-E3 was prepared following the double impregnation method with an intermediate heating step, as reported elsewhere for sucrose [3], but using ultrasound for mixing the xylose extract solution with the SBA-15 instead of conventional magnetic stirring. The appropriate amount of xylose extract solution (equivalent to half the total carbon/SBA-15 ratio) was mixed with 1 g of SBA-15 under ultrasound for 10 min. The mixture was placed in a crucible and heated in a muffle at 100 °C for 6 h and at 160 °C for 6 h. After grinding the material, the impregnation process was repeated with the addition of the rest of the amount of the xylose extract, (equivalent to half the total carbon/SBA-15 ratio). Carbonization, template removal and subsequent washing-drying steps were carried out under the same conditions as the rest of the samples. Table 1 summarizes the preparation conditions of the carbons.

2.2.3. Preparation of ordered mesoporous carbons from glucose

Three samples were prepared with commercial glucose and two with glucose extract obtained from almond shells (Table 1).

For preparing sample *C*-Glu-C1, 6 g of commercial xylose was dissolved in 5 mL of distilled water. Then, 0.2 g of concentrated sulfuric acid and 1 g of SBA-15 were added and stirred with ultrasound for 10 min. The mixture was rota-evaporated under vacuum at 50 °C. The sample was completely dried in an oven. The solid obtained was carbonized in a quartz reactor with a nitrogen flow of 100 mL/min at 900 °C for 4 h. The material was ground to obtain a homogenous powder. The elimination of the template SBA-15 was performed by refluxing the carbonized material with 100 mL of 0.625 M NaOH (≥98%, Merck) at 90 °C for 24 h. The resulting solid was filtered, washed with distilled water repeatedly until neutral pH, and finally dried in an oven.

Two more samples were prepared following the double impregnation method with an intermediate heating step, as reported elsewhere for sucrose [3], without using or using ultrasounds for mixing the reagents (samples *C*-Glu-C2 and *C*-Glu-C3, respectively). For preparing *C*-Glu-C2, 2 g of commercial glucose was dissolved in 5 mL of distilled water. Then, 0.2 g of concentrated sulfuric acid (98 wt %, Scharlau) and 1 g of SBA-15 were added and stirred for 2 h with magnetic stirring. The mixture was heated in a muffle at 100 °C for 6 h and at 160 °C for 6 h. After grinding the solid, the impregnation process was repeated with the addition of 2 more g of glucose dissolved in 5 mL of distilled water. Carbonization, elimination of the template and later washing-drying procedures were carried out at the same conditions as for the sample *C*-Glu-C1. Sample *C*-Glu-C3 was prepared following the same procedure as *C*-Glu-C2 but

Table 1
Preparation conditions of the ordered mesoporous carbon materials.

Samples	Carbon precursor (CP)	CP/SBA-15 wt ratio	Preparation conditions	Carbonization conditions
C-Xyl-C1	commercial xylose	6:1	Solid state	650 °C/2 h
C-Xyl-C2	commercial xylose	6:1	Impregnation/H_2SO_4/US/	650 °C/2 h
C-Xyl-E1	xylose extract	6:1	Impregnation/US/heating step at 100 °C & 160 °C	650 °C/2 h
C-Xyl-E2	xylose extract	6:1	Impregnation/US	650 °C/2 h
C-Xyl-E3	xylose extract	6:1	Double Impregnation/US/heating step at 100 °C & 160 °C	650 °C/2 h
C-Glu-C1	commercial glucose	4:1	Impregnation/US	900 °C/4 h
C-Glu-C2	commercial glucose	4:1	Double impregnation/H_2SO_4/heating step at 100 °C & 160 °C	900 °C/4 h
C-Glu-C3	commercial glucose	4:1	Double impregnation/H_2SO_4/US/heating step at 100 °C & 160 °C	900 °C/4 h
C-Glu-E1	glucose extract	4:1	Impregnation/US	900 °C/4 h
C-Glu-E2	glucose extract	4:1	Double Impregnation/US/heating step at 100 °C & 160 °C	900 °C/4 h
C-Lig-E1	lignin extract 1	3:1	Impregnation/US	650 °C/2 h
C-Lig-E2	lignin extract 1	2:1	Impregnation/US	650 °C/2 h
C-Lig-E3	lignin extract 1	2:1	Impregnation/US	900 °C/4 h
C-Lig-E4	lignin extract 1	2:1	H_2SO_4[a]/US/heating step at 100 °C & 160 °C	650 °C/2 h
C-Lig-E5	lignin extract 1	2:1	H_2SO_4[b]/US/heating step at 100 °C & 160 °C	650 °C/2 h
C-Lig-E6	lignin extract 2	2:1	Impregnation/US	650 °C/2 h

[a] Sulfuric acid was added to the starting lignin/SBA-15 mixture.
[b] Sulfuric acid was added to the lignin/SBA-15 mixture previously dried. US: ultrasounds. CP: carbon precursor.

applying ultrasounds to the mixture of glucose, sulfuric acid, and SBA-15 for 10 min for each impregnation to favor the diffusion of the carbon source into the pores of the SBA-15.

Finally, two samples were prepared at similar conditions as those used for preparing samples *C*-Glu-C1 and *C*-Glu-C3 but using glucose extract solution in the appropriate amounts to have the same carbon precursor/SBA-15 ratio (samples *C*-Glu-E1 and *C*-Glu-E2, respectively), and without adding sulfuric acid since the glucose extract was already acid because of the methodology used to obtain it. Carbonization, template removal, and later washing-drying of these samples were carried out at the same conditions as that used for the rest of the samples prepared with glucose.

2.2.4. Preparation of ordered mesoporous carbons from lignin

Several samples were prepared using the lignin extract solution 1, obtained from almond shells, by changing the preparation conditions and one more was prepared with the lignin extract solution 2, which was also obtained from almond shells but with higher lignin concentration (Table 1).

Samples *C*-Lig-E1 and *C*-Lig E2 were prepared by impregnation with a carbon precursor/template weight ratio of 3 and 2, respectively (Table 1). The appropriate amount of lignin extract 1 was mixed with 2 g of SBA-15 applying ultrasounds for 10 min to favor homogenization, and then, dried in an oven at 80 °C overnight. The solids obtained were carbonized in a quartz reactor with a nitrogen flow of 100 mL/min at 650 °C for 2 h. The materials were ground to obtain a homogenous powder. The elimination of the template SBA-15 was performed by refluxing the carbonized material with 100 mL of 0.625 M NaOH at 90 °C for 24 h. Samples were filtered, washed with distilled water until neutral pH, and finally dried in an oven. Sample *C*-Lig-E3 was prepared at the same conditions as those of sample *C*-Lig-E2 but the carbonization step was made in a quartz reactor with a nitrogen flow of 100 mL/min at 900 °C for 4 h.

Other two samples, *C*-Lig-E4 and *C*-Lig-E5 were synthesized by adding 0.4 g of concentrated sulfuric acid to the mixture at different points of the preparation step. For sample *C*-Lig-E4, sulfuric acid was added to the initial mixture of lignin extract and SBA-15 and dried at 80 °C in an oven overnight. Then, the solid was ground, and 5 mL of deionized water was added while applying ultrasounds for 10 min until obtaining a thick paste. This paste was heated in a muffle at 100 °C for 6 h and at 160 °C for 6 h. For *C*-Lig-E5, first, the lignin extract and the SBA-15 were mixed by applying ultrasounds for 10 min, and the mixture was dried in an oven at 80 °C overnight. Then, the dried solid was ground and transferred into a crucible where 0.4 g of sulfuric acid and 5 mL of water were added and mixed with ultrasounds for 5 min until forming a thick paste. This paste was heated in a muffle at 100 °C for 6 h and at 160 °C for 6 h. Carbonization, template removal and later washing-drying procedures were carried out at the same conditions as those used for the samples *C*-Lig-E1 and *C*-Lig-E2 (Table 1).

Finally, one sample was prepared at the same conditions as sample *C*-Lig-E2 but using lignin extract solution 2, which was more concentrated, instead of lignin extract solution 1.

2.3. Preparation of the catalysts

2.3.1. Preparation of sulfonic-acid functionalized OMC catalysts

SO_3H-OMC samples were prepared from OMCs obtained from xylose, glucose and lignin extracts. 0.7 g of OMC was treated with 25 mL of concentrated sulfuric acid under refluxing at 80 °C for 2 h (named as S2) or for 24 h (named as S24). Then, the mixture was filtered and washed with hot distilled water until neutral pH. To neutralize harmful gases, a gas wash bottle system with NaOH solution was used. The sulfonic acid-functionalized ordered mesoporous carbons were dried overnight at 80 °C. Two SO_3H-OMC were prepared from *C*-Xyl-E2 (S2–*C*-Xyl-E2 and S24–*C*-Xyl-E2), one from *C*-Glu-E2 (S24–*C*-Glu-E2) and two more from *C*-Lig-E2 (S2–*C*-Lig-E2 and S24–*C*-Lig-E2).

2.3.2. Preparation of Ni/OMC catalysts

Ordered mesoporous carbons *C*-Lig-E2 and *C*-Lig-E6, obtained from lignin extract 1 and 2, respectively, were mixed with 25 mL of an ethanolic solution containing the appropriate amount of $Ni(NO_3)_2{\cdot}6H_2O$ (Extrapure, Scharlau) to have a 28 wt % of metallic Ni in the final catalyst. Then, the solvent was rotary-evaporated. The resulting solid was dried at 80 °C overnight and calcined under nitrogen atmosphere flow (100 mL/min) at 450 °C for 2.5 h (Ni/C-Lig-E2 and Ni/C-Lig-E6). Synthesized H-Beta was added to Ni–*C*-Lig-E2 and Ni–*C*-Lig-E6, and different amounts of the acid-functionalized ordered mesoporous carbons S2–*C*-Lig-E2 and S24–*C*-Lig-E2 were added to Ni–*C*-Lig-E2 to provide Brønsted acidity to the catalytic systems. H-Beta was prepared by treating commercial Na-Beta zeolite (Zeochem, Si/Al = 10, PB Lot No. 6000186) with NH_4NO_3 1 M at 100 °C for 1 h. Then, the sample was washed several times with deionized water and calcined at 540 °C for 5 h.

2.4. Characterization techniques

X-ray diffraction was used to identify and quantify the crystalline phases present in the samples. The experiments were carried out with a

Siemens D5000 diffractometer (Bragg–Brentano parafocusing geometry and vertical θ–θ goniometer) fitted with a curved graphite diffracted-beam monochromator and diffracted-beam Soller slits, a 0.06° receiving slit and scintillation counter as a detector. The angular 2θ diffraction range was between 0.5 and 5° for the SBA-15 and OMC samples and from 5 to 80° for the Ni/OMC catalysts. The sample was dusted onto a low background Si (510) sample holder. The data were collected with an angular step of 0.05° at 3 s per step and sample rotation. CuKα radiation was obtained from a copper X-ray tube operated at 40 kV and 30 mA. The crystalline phases were identified by cross-comparison of the diffractogram of the sample with reference data from the International Center for Diffraction Data. The JCPDS files used for the identification of the crystalline phases in samples Ni/C-Lig-E2 and Ni/C-Lig-E6 were 01-077-9326 and 00-047-1049 for Ni and NiO (bunsenite), respectively. The relative quantitative phase analysis was obtained for these Ni/OMC catalysts by refining the Rietveld scale factor for each phase and applying the corresponding well-known equations [31]. The peak width of each phase was modelled with the Double-Voigt Approach by considering only the Lorentzian contribution of the crystallite size effect and discarding any contribution of the microstrain to the peak width [32]. The averaged integral breadth was obtained from the resulting fitted Voigt function to the whole diffractogram.

BET surface areas were calculated from the nitrogen adsorption isotherms at −196 °C using a Quantachrome Quadrasorb SI surface analyzer and a value of 0.164 nm^2 for the cross-section of the nitrogen molecule. Pore size distribution was obtained from the desorption results of the isotherm by applying the BJH method.

Thermogravimetric analysis (TGA) was employed to determine the carbon content of the OMC materials. Experiments were performed by heating at 10 °C/min from 30 °C to 800 °C under an airflow rate of 50 mL/min in Mettler Toledo TGA 2 equipment. Carbon content was calculated by the difference between the initial sample weight and the final residual weight. Thermogravimetric analysis technique was also used to confirm and quantify the introduction of the sulfonic acid groups (sulfur content) for the sulfonic acid-functionalized samples since the weight loss observed around 300 °C in the TGA has been related in the literature to the loss of these sulfonic acid groups [33]. Thermogravimetric analysis was performed from 25 °C to 900 °C at 10 °C/min under nitrogen flow. To identify the exact interval due to the sulfonic groups, the TGA of the corresponding OMC without sulfonation was performed at the same conditions.

TEM characterization of the samples was done using a JEOL 1011 transmission electron microscope operating at an accelerating voltage of 100 kV and magnification of 120–400 k. The sample powder (0.1 mg) was dispersed in ethanol (50 μL) by using ultrasounds. Then, the suspension was placed on a carbon-coated copper grid and air dried.

SEM was used to observe the morphology and particle sizes of the samples. Experiments were performed on a scanning electron microscope, JEOL JSM6400, operating at accelerating voltage of 5 kV, work distances of 10 mm, and magnifications of 12,000–20000*X*.

The Brønsted acid capacity of the acid functionalized samples was measured through the determination of cation exchange capacities using aqueous sodium chloride (2 M) solutions as a cationic exchange agent. The released protons were then titrated [34].

The Boehm method was applied to determine the content of acidic and basic functional groups on the surface of several representative OMC samples following the procedure reported elsewhere [35]. 50 mL of 0.01 N of the base solutions (Na_2CO_3, $NaHCO_3$ and NaOH) were added to 120 mg of sample *C*-lig-E6, 150 mg of sample *C*-glu-E2 and 200 mg of *C*-Xyl-E2. The mixtures were stirred for 48 h 50 mL of each solution was also transferred in similar beakers without carbon (Reference samples). Reference samples were treated exactly as the current samples. After 48 h, the samples were vacuum filtered. A 10 mL aliquot was taken and transferred to another beaker, and 20 mL of HCl 0.01 N was added before titration with Na_2CO_3 0.01 N.

2.5. Catalytic activity

2.5.1. Catalytic etherification of glycerol with isobutene to di- and triethers of glycerol (h-GTBE)

Etherification experiments were performed in a stainless-steel stirred autoclave (150 mL) at 80 °C for 24 h or 48 h. Stirring was fixed for all experiments at 1000 rpm to avoid external diffusion limitations. Typically, the composition of the reaction mixture was: 10 g glycerol (≥99%, Honeywell Research Chemicals), glycerol/isobutene (≥99.5%, Linde Gas) ratio of 1:4 and 5 wt % of catalyst.

The reaction products were analyzed by gas chromatography in a Shimadzu GC-2010 equipped with a SupraWax-280 column and a FID detector. 1-butanol (99 %, SDS) was used as an internal standard. Glycerol conversion and selectivity to glycerol monoethers (MTBG) were determined from calibration curves obtained from commercial products. For glycerol diethers (DTBG) and triether (TTBG), which were not available commercially, we isolated them from the reaction products by column chromatography and identified them by ^{13}C and ^{1}H NMR for proper quantification [36]. Turnover frequency values (TOF) were calculated as moles of glycerol converted per mole of active species (H^+) per hour. Reproducibility of the catalytic results for the best OMC catalyst was studied by testing it thrice at the same reaction conditions.

2.5.2. Catalytic obtention of levulinic acid from 5-hydroxymethyl furfural (5-HMF)

Catalytic transformation of 5-hydroxymethyl furfural (≥99%, Merck) to levulinic acid was performed in a stainless-steel stirred autoclave (50 mL) at 160 or 180 °C for 1 h 15 min. Stirring was fixed for all experiments at 1000 rpm, and water or γ-valerolactone (99 %, Merck):water mixture (25:75) were used as solvents. For each experiment, 1 g of 5-HMF and 25 wt% of catalyst were used. The reaction products were identified by gas chromatography in a Shimadzu GC-2010 instrument equipped with a column Suprawax-280 (60 m × 0.25 mm x 0.50 μm) and a FID detector. 1-Butanol (99 %, SDS) was the internal standard. The quantification of the products to calculate conversion and selectivity was determined from calibration curves obtained from commercial products. Turnover frequency values (TOF) were calculated as moles of glycerol converted per mole of active species (H^+) per hour. Reproducibility of the catalytic results for the best OMC catalysts was studied by testing them thrice at the same reaction conditions.

2.5.3. Hydrodeoxygenation of guaiacol

Hydrodeoxygenation of guaiacol (≥98%, Alfa Aesar Chemicals) was performed in a stainless-steel stirred autoclave (150 mL) at 180 °C, 30 bars H_2 for 1 h. Stirring was fixed for all experiments at 1000 rpm to avoid external diffusion limitations. Typically, the reactor was filled with 200 mg of guaiacol, 40 mL of n-dodecane (99%, Thermo Fisher Scientific) and 100 mg of catalyst Ni/C-Lig-E2. In some experiments, 100 or 300 mg of H-Beta or S2–*C*-Lig-E2 or S24–*C*-Lig-E2 were combined by physical mixing with 100 mg of Ni/C-Lig-E2. In another catalytic experiment, 100 mg of catalyst Ni/C-Lig-E6 was mixed with 100 mg of H-Beta.

The identification and quantification of the reaction products was performed by gas chromatography in a Shimadzu GC-2010 instrument equipped with a column TRB-PETROL (100 m × 0.25 mm x 0.50 μm) and a FID detector using calibration lines obtained from commercial products. Hexadecane (99 %, Alfa Aesar Chemicals) was the internal standard. Reproducibility of the catalytic results for the best OMC catalyst was studied by checking it thrice.

3. Results and discussion

3.1. Characterization of the SBA-15

The low-angle XRD pattern of the SBA-15 sample, which was used as a template for the preparation of OMCs, showed three peaks

corresponding to the 100, 110 and 200 reflections of the ordered 2D hexagonal (*P6mm*) mesostructure (Fig. 1a), as confirmed by TEM in which the mesoporous channels in the hexagonal arrangement were perfectly observed (Fig. 1b). N_2 adsorption-desorption isotherm of the SBA-15 was of type IV, which corresponded to mesoporous materials, according to the Brunauer, Emmett and Teller classification. (Fig. 1c). The sample showed a narrow unimodal pore size distribution with a maximum at around 70 Å. (Fig. 1c). The BET surface area for this sample was 868 m^2/g.

3.2. Characterization of the OMC samples

3.2.1. Preparation of ordered mesoporous carbons from xylose

All the XRD patterns of the carbons prepared from xylose showed the main peak corresponding to the 100 reflection with high intensity (Fig. 2a). Additionally, for the samples *C*-Xyl-C1, obtained from commercial xylose, and *C*-Xyl-E2, obtained from xylose extract, the peaks due to the 110 and 200 reflections were also clearly detected while for the rest of the samples (*C*-Xyl-C2, *C*-Xyl-E1 and *C*-Xyl-E3) they can be intuited but with much less resolution. This means that a higher ordering of the structure was achieved for the carbons *C*-Xyl-C1 and *C*-Xyl-E2. TEM micrographs of the carbons confirmed the successful replica of the hexagonal structure of SBA-15, as shown in Fig. 2, in which the channels characteristic of these ordered mesoporous materials were perfectly observed.

The differences observed between the diffractograms of the carbons obtained from commercial xylose could be explained by the higher contact between the xylose and the SBA-15 template in solid state for *C*-Xyl-C1, which could favor a more uniform diffusion of the carbon precursor into the pores of the SBA-15. For the samples prepared from xylose extract, better definition of the XRD peaks was obtained for *C*-Xyl-E2, prepared by impregnation with ultrasounds and later rotaevaporation. The double impregnation with the intermediate heating step did not improve the definition of the small peaks although it had also high crystallinity (*C*-Xyl-E3). Therefore, the incorporation of the xylose extract, obtained from almond shells, can lead to the formation of OMCs at low carbonization temperature (650 °C).

Table 2 shows the BET surface area values, obtained from nitrogen physisorption, and the % C content, determined by thermogravimetry, for all samples. Carbons obtained from xylose exhibited isotherms type IV corresponding to mesoporous materials, high surface BET areas and high C content. On the whole, the carbons with higher crystallinity had slightly lower surface areas.

3.2.2. Preparation of ordered mesoporous carbons from glucose

Fig. 3 shows the XRD patterns of the carbons prepared from commercial and extracted glucose, and the TEM images of several samples.

XRD of the carbons clearly exhibited a high-intense peak

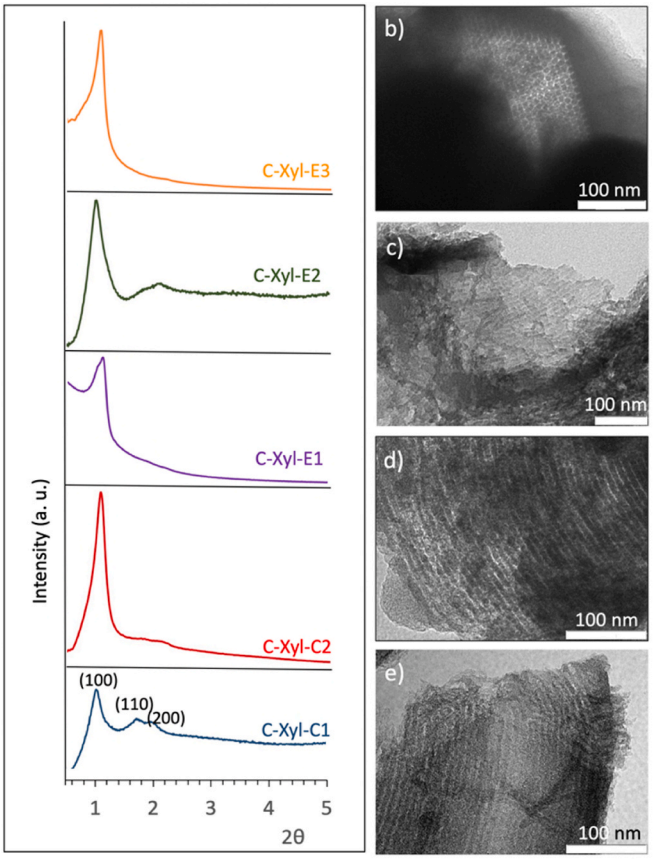

Fig. 2. a) X-ray diffraction patterns of the ordered mesoporous carbons obtained from commercial and xylose extract; Transmission electron micrographs of b) *C*-Xyl-C1, c) *C*-Xyl-E1, d) *C*-Xyl-E2, and d) *C*-Xyl-E3.

corresponding to the 100 reflection. Additionally, the peaks due to the 110 and 200 reflections can be slightly appreciated for all of them (Fig. 3a). This confirms the hexagonal structure of the OMCs materials synthesized with the inverse structure of the SBA-15, as observed by TEM where the characteristic channels of these ordered mesoporous materials were perfectly visualized (Fig. 3b, c and d). The use of a higher carbonization temperature (900 °C) for preparing these samples resulted in carbons with higher ordering, as expected.

By comparing the diffractograms of the samples obtained from commercial glucose, the use of double impregnation with an intermediate heating step in the presence of ultrasounds (*C*-Glu-C3) led to the highest crystallinity although the definition of the small peaks was similar (Fig. 3). The addition of sulfuric acid during the impregnation of

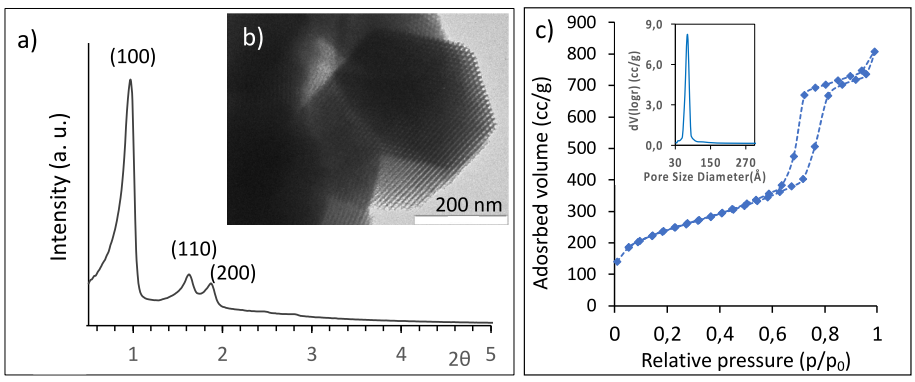

Fig. 1. a) X-ray diffraction pattern, b) Transmission electron micrography and c) Nitrogen adsorption-desorption isotherm of the template SBA-15 and pore size distribution graphic.

Table 2
Characterization of the OMCs.

Samples	C content[a] (%)	BET surface area[b] (m^2/g)
C-Xyl-C1	94	576
C-Xyl-C2	96	610
C-Xyl-E1	90	680
C-Xyl-E2	96	651
C-Xyl-E3	91	672
C-Glu-C1	90	719
C-Glu-C2	98	749
C-Glu-C3	96	735
C-Glu-E1	95	806
C-Glu-E2	95	786
C-Lig-E1	92	902
C-Lig-E2	98	785
C-Lig-E3	90	725
C-Lig-E4	98	813
C-Lig-E5	96	948
C-Lig-E6	93	711

[a] Determined by thermogravimetry.
[b] Determined by N_2 physisorption.

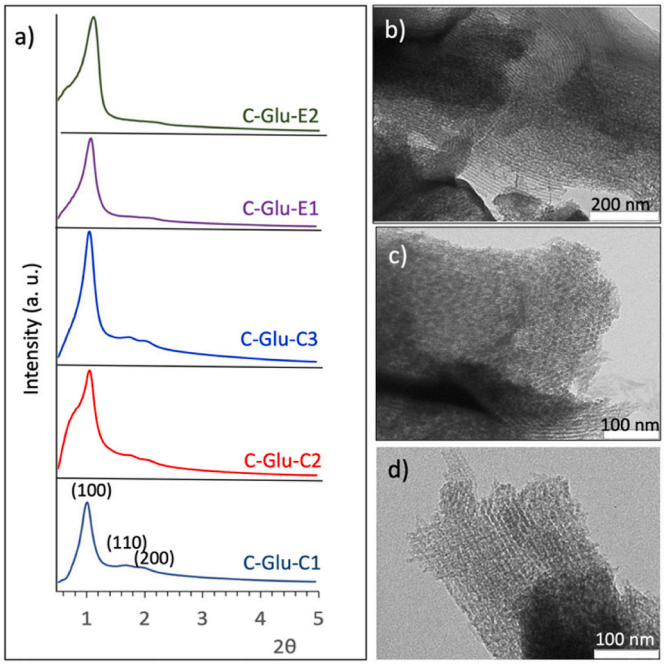

Fig. 3. a) X-ray diffraction patterns of the ordered mesoporous carbons obtained from commercial and glucose extract; Transmission electron micrographs of b) *C*-Glu-C2, c) *C*-Glu-E1 and d) *C*-Glu-E2.

glucose favored the polymerization-carbonization reaction [3], and the ultrasounds favored the diffusion of the glucose inside the pores of the mesoporous silica. The carbons prepared from the glucose extract solution, obtained from biomass, showed slightly lower crystallinity than those prepared from commercial glucose (Fig. 3).

All carbons exhibited isotherms type IV corresponding to mesoporous materials, high surface BET areas and high C content after template elimination (Table 2).

3.2.3. *Preparation of ordered mesoporous carbon from lignin*

Fig. 4 shows the XRD patterns and several TEM images for the carbons prepared from lignin. Different parameters were modified using lignin extract 1 to optimize the conditions of preparation since, to our knowledge, there are no references in the literature about the obtention of OMCs from lignin by the hard template methodology. We only found OMCs prepared via soft-templating using Pluronic F127 as template and

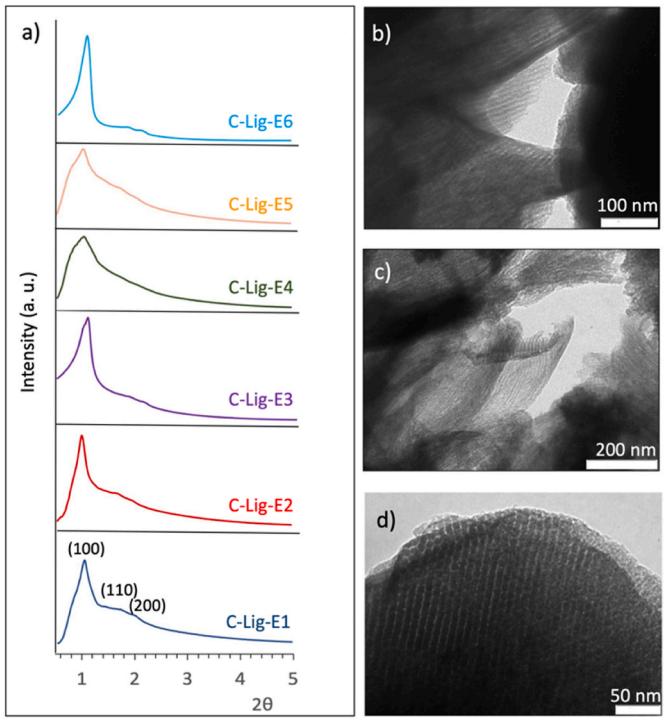

Fig. 4. a) X-ray diffraction patterns of the ordered mesoporous carbons obtained from lignin and SBA-15; Transmission electron micrographs of b) *C*-Lig-E2, c) *C*-Lig-E4, and d) *C*-Lig-E6.

lignin sources such as walnut shell, macadamia nutshell, tobacco stem, hardwood or kraft [37–40].

The first idea was to use lower carbon precursor/SBA-15 ratios than for carbohydrates considering the polymeric structure of the lignin. Ultrasound were applied for all samples to favor the access of lignin to the template pores.

XRD patterns of samples *C*-Lig-E1 and *C*-Lig-E2, prepared with lignin/template wt ratio of 3 and 2, respectively, were similar with the presence of the most intense peak due to the 100 reflection. Additionally, the peaks corresponding to the 110 and 200 reflections can be slightly appreciated. However, sample *C*-Lig-E2 showed a more well-defined and regular 100 reflection peak. XRD pattern of sample *C*-Lig-E3, synthesized at the same preparation conditions as *C*-Lig-E2 but carbonized at higher calcination temperature (900 °C), showed higher definition especially for the 100 reflection peak. This confirms the effect of the carbonization temperature on the crystallinity of the carbons.

When sulfuric acid was added at different steps of the OMC preparation (*C*-Lig-E3 and *C*-Lig-E4), as previously done for the OMCs obtained from xylose and glucose, the peak due to reflection 100 was observed but with much lower crystallinity than for the samples prepared without an acidic medium. This confirms that for carbohydrates (glucose and xylose), the presence of an acid medium favors their polymerization, and therefore, the formation of the OMCs while when using lignin, it is not necessary since lignin is already a polymer.

Interestingly, by using lignin extract 2, with a higher concentration than lignin extract 1, at the same preparation conditions as *C*-Lig-E2, including carbonization at 650 °C for 2 h, the crystallinity of the resulting sample, *C*-Lig-E6, much higher with a higher resolution of the peaks (Fig. 4a). Therefore, the concentration of the lignin extract used for impregnation has been shown to be a key factor for obtaining highly-ordered mesoporous carbons. This effect was not observed for xylose and glucose.

TEM micrographies of several *C*-Lig samples allowed us to observe the characteristic channels of these ordered mesoporous carbons (Fig. 4 b, 4c and 4 d). All samples exhibited isotherms type IV corresponding to

mesoporous materials, high surface BET areas and high C content (Table 2).

3.2.4. Comparison of the surface properties for three representative ordered mesoporous carbons, obtained from xylose, glucose and lignin extracts

Pore size distribution graphic of three representative OMCs, obtained from xylose (*C*-Xyl-E2), glucose (G-Glu-E2), and lignin (*C*-Lig-E2) confirmed the presence of mesopores with a diameter smaller (around 35 Å) (Fig. 5) than in the template (70 Å) (Fig. 1c), as expected.

Scanning electron micrographies of the ordered mesoporous carbons mostly maintained the morphology and homogeneity of the rod shape particles of the SBA-15 template, with less definition, and with sizes around 1–3 μm (Fig. 6).

The Boehm method was applied to study the surface content of acidic and basic functional groups for these representative OMCs (Table 3). According to the literature, carboxylic acids decompose as CO_2 below 400 °C, the presence of lactones can be observed above 600 °C and the phenol groups are decomposed in a middle temperature range (500–750 °C) [41]. The three OMCs had low surface oxygenated groups, as expected, since no oxidation treatment was performed prior to their determination. However, the OMC obtained from lignin (*C*-lig-E2) exhibited the highest contribution of phenolic groups. This means that, among the surface groups present in the starting lignin fraction, such as hydroxyl groups in alcohol and phenolic forms, carbonyl groups, carboxyl groups or methoxyl groups, some phenolic groups could persist under the preparation and carbonization conditions used to obtain this green OMC [41]. The slightly number of phenols detected for the *C*-Xyl-E2 sample, obtained from xylose, could be related to the presence of some lignin in the sample, considering the extraction process followed.

3.3. Characterization of sulfonic acid-functionalized OMC catalysts

After treatment with sulfuric acid, the ordered mesoporous carbons showed a significant decrease of the surface area (Table 4 vs Table 2) accompanied by a decrease in the crystallinity of the samples although the structure remained, as confirmed by XRD (Fig. 7a), TEM (Fig. 7b and c), and nitrogen physisorption results (Fig. 7d), in which the isotherms were of type IV in spite of the decrease of the adsorbed volume.

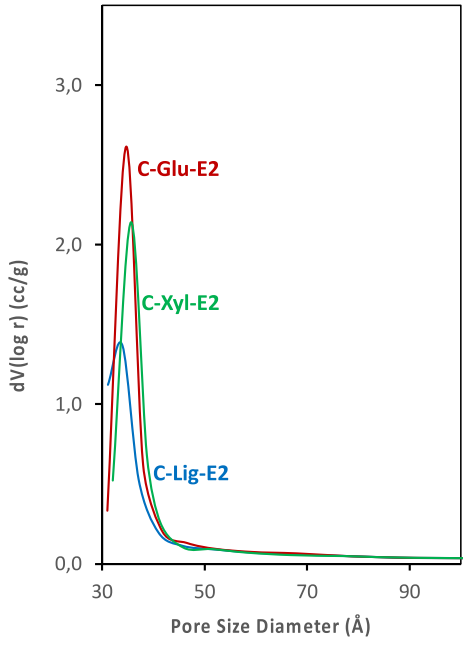

Fig. 5. Pore size distribution graphic of three representative ordered mesoporous carbons obtained from xylose, glucose and lignin.

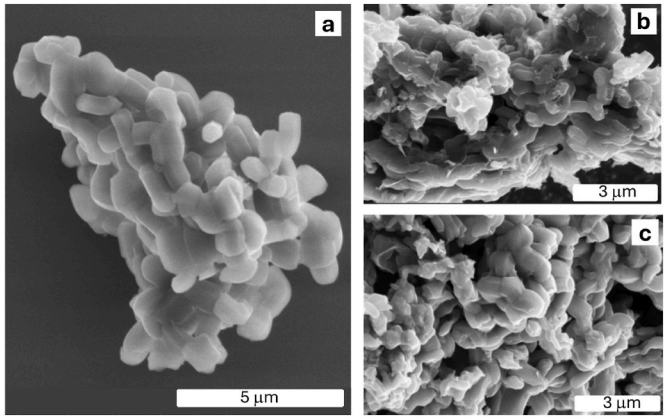

Fig. 6. Scanning electron micrographs of the samples: a) SBA-15, b) *C*-Xyl-E2, and c) *C*-Lig-E2.

Table 3
Characterization of the surface acidic and basic functional groups of three representative OMCs by the Boehm method.

Samples	Carboxyl groups (mmol/g)	Lactones (mmol/g)	Phenols (mmol/g)
C-Xyl-E2	0.012	0.024	0.074
C-Glu-E2	0.032	0.016	0.000
C-Lig-E2	0.061	0.019	0.220

Table 4
Characterization of the SO_3H-OMC catalysts.

Samples	BET surface area[a] (m^2/g)	Acid capacity[b] (meq H^+/g)	Sulfur content[c] (mmol sulfonic acid group/g sample)
S2–*C*-Xyl-E2	304	0.64	0.73
S24–*C*-Xyl-E2	271	0.97	1.11
S24–*C*-Glu-E2	402	0.62	0.72
S2–*C*-Lig-E2	397	0.19	0.24
S24–*C*-Lig-E2	376	0.21	0.26

[a] Determined by N_2 physisorption.
[b] Obtained by potentiometric titration.
[c] Calculated from thermogravimetry.

Thermogravimetric analysis of the sulfonated samples showed a weight loss between 200 °C and 360 °C related to the incorporation of the sulfonic groups (Fig. 8), in agreement with the literature [34]. The sulfur content was calculated from TGA results and is indicated in Table 3. Higher amount of Brønsted acid sites were incorporated by treating the *C*-Xyl-E2 carbon with sulfuric acid at longer time, as deduced from titration results (Table 4). This confirms the results obtained by TGA. In contrast, longer time of sulfuric acid treatment of *C*-Lig-E2 practically did not improve the incorporation of the sulfonic groups (Table 4). These differences could be related to the presence of different chemical species on the surface of the OMC, depending on the biomass fraction precursor used, which favored or difficulties the incorporation of the sulfonic groups.

3.4. Characterization of Ni/OMC catalysts

Fig. 9a shows the XRD pattern of the Ni/C-Lig-E2 catalyst, obtained by calcination of the ordered mesoporous carbon *C*-Lig-E2 impregnated

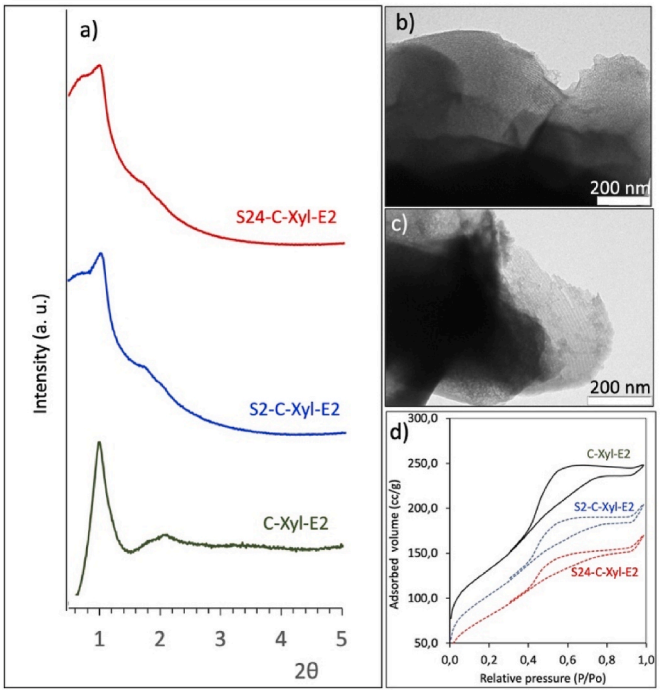

Fig. 7. a) X-ray diffraction patterns and b) nitrogen adsorption-desorption isotherms of the sulfonated samples S2–*C*-Xyl-E2 and S24–*C*-Xyl-E2 compared to the starting carbon *C*-Xyl-E2; and transmission electron micrographs of the c) carbon *C*-Xyl-E2, and d) sulfonated carbon S24–*C*-Xyl-E2.

with nickel nitrate, at 450 °C for 2.5 h under nitrogen flow. Interestingly, metallic Ni was identified as the main crystalline phase (83 %). Additionally, NiO was observed in low amounts (17 %). This means that OMC played the role of reducing agent. This effect was confirmed when obtaining at the same calcination conditions catalyst Ni/C-Lig-E6, in which metallic Ni was again the major phase (93 %) in addition to the detection of small amounts of NiO (7 %).

TEM micrographies of these catalysts exhibited a good dispersion of the Ni nanoparticles (10–25 nm) on the mesoporous carbons in which channels were still observed (E.g. Fig. 9b). Nitrogen physisorption showed an isotherm of type IV and unimodal pore size distribution with a maximum around 40 Å, corresponding to mesoporous materials (E.g. Fig. 9c). However, a decrease in the volume of adsorbed nitrogen, and consequently, lower surface areas were observed for Ni/C-Lig-E2 (458 m^2/g) and Ni/C-Lig-E6 (397 m^2/g) with respect to their corresponding supports, *C*-Lig-E2 (785 m^2/g) and *C*-Lig-E6 (711 m^2/g), respectively. This can be explained by the partial blockage of the pores by the Ni particles.

Table 5 depicts the BET surface area values and the amount of Brønsted acid sites of the two Ni/OMC catalysts and several physical mixtures prepared with acid materials. All mixtures maintained the type IV nitrogen isotherm shape and the unimodal pore size distribution (e.g. Fig. 9c). Ni/C-Lig-E2 and Ni/C-Lig-E6 showed very low acidity, as expected, while the mixtures had surface areas and amount of Brønsted acid sites in values between those that the starting materials have. For example, Ni/C-Lig-E2 + H-Beta, obtained by physical mixture of 100 mg of each one, had surface area and acidity values between those of Ni/C-Lig-E2 and H-Beta (579 m^2/g, 0.60 mmol H^+/g).

3.5. Catalytic activity

3.5.1. Catalytic etherification of glycerol with isobutene to h-GTBE using sulfonated OMCs obtained from xylose extract

Catalytic etherification of glycerol with isobutene to obtain h-GTBE is a consecutive reaction of transformation of glycerol to monoether, monoether to diethers, and, finally, diethers to triether (Scheme 1a). In previous works on this reaction, we concluded that the number and strength of Brønsted acid sites, the accessibility of the reactants to the active sites, which depends on the pore size rearrangement and the surface area, in addition to the reaction time affect the selectivity to the h-GTBE [14–17].

Fig. 10 shows the catalytic activity results obtained using the sulfonic acid-functionalized ordered mesoporous carbons obtained from xylose extract (S2–*C*-Xyl-E2 and S24–*C*-Xyl-E2) for the etherification of glycerol with isobutene. Commercial sulfonic macroporous resin Amberlyst-15 (A15) was also tested for comparison (surface area of 39 m^2/g and 4.70 mmol H^+/g). TOF values are indicated in the Figure divided by 10 to better observe the differences between catalysts. The reaction products obtained were *mono-tert*-butyl glycerol ether (MTBG), *di-tert*-butyl glycerol ether (DTBG) and *tri-tert*-butyl glycerol ether (TTBG). Additionally, diisobutylene (DIB), produced by dimerization of the remaining isobutylene, was detected in low amounts for the sulfonated OMC catalysts (1–5 wt %) in contrast to the higher amounts (35 wt %)

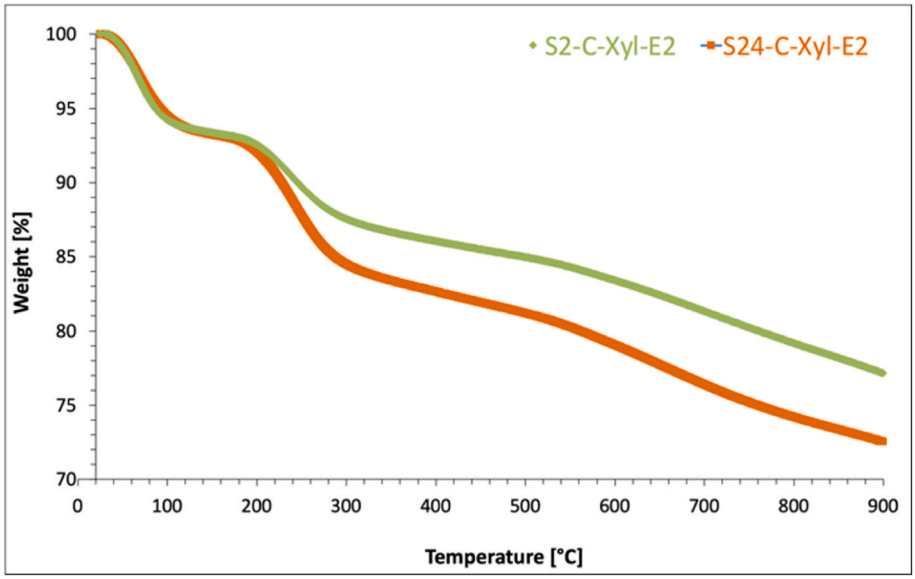

Fig. 8. Thermogravimetry curves of sulfonated ordered mesoporous carbons S2–*C*-Xyl-E2 and S24–*C*-Xyl-E2.

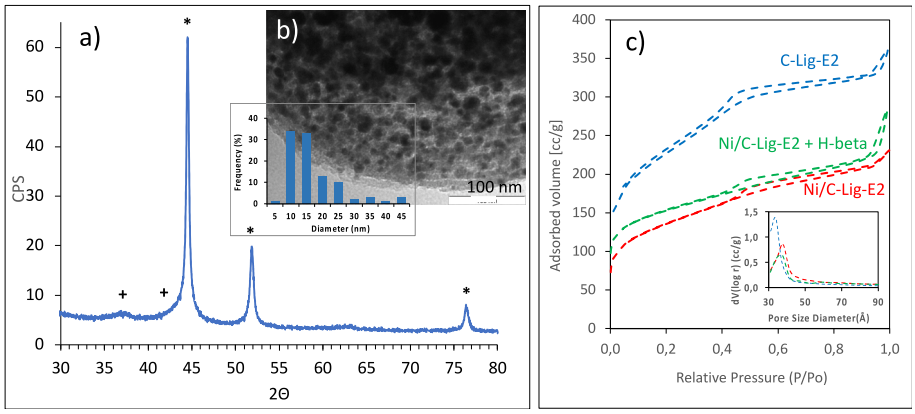

Fig. 9. a) X-ray diffraction pattern and b) transmission electron micrograph of the catalyst Ni/C-Lig-E2, and its Ni particle size distribution graphic, and c) Nitrogen adsorption-desorption isotherms and pore size distribution graphic of *C*-Lig-E2, Ni/C-Lig-E2 and Ni/C-Lig-E2 + H-Beta. * Ni phase; + NiO phase.

Table 5
Characterization of the Ni/OMC catalysts.

Catalysts	BET surface area[a] (m^2/g)	Acid capacity[b] (meq H^+/g)
Ni/C-Lig-E2	458	0.06
Ni/C-Lig-E2+S2–*C*-Lig-E2	357	0.09
Ni/C-Lig-E2+S24–*C*-Lig-E2	342	0.10
Ni/C-Lig-E2+S2–*C*-Lig-E2 (300 mg)	137	0.12
Ni/C-Lig-E2+S-Beta	330	0.32
Ni/C-Lig-E2+H-Beta	499	0.23
Ni/C-Lig-E6	397	0.05
Ni/C-Lig-E6 +H-Beta	436	0.20

[a] Determined by N_2 physisorption.
[b] Obtained by potentiometric titration.

obtained for Amberlyst-15. These non-desired byproducts can be problematic when formulated with fuels. All sulfonated catalysts maintained the sulfur content after the reaction, as determined by TGA. This confirms that there was no leaching of the sulfonic acid groups during the reaction.

Catalysts S2–*C*-Xyl-E2 and S24–*C*-Xyl-E2, obtained after impregnation of *C*-Xyl-E2 with H_2SO_4 at 80 °C for 2 and 24 h, respectively, showed low conversion (6–24 %) and low selectivity to the desired products (h-GTBE) (8–17 %) with no detection of TTBG after 24 h of reaction. The slightly higher activity values observed for S24–*C*-Xyl-E2 when compared to S2–*C*-Xyl-E2 can be explained by its higher amount of Brønsted acid sites (Table 4). Interestingly, S24–*C*-Xyl-E2 had comparable TOF value to Amberlyst-15 although leading much lower conversion (Fig. 10). This means that although S24–*C*-Xyl-E2 had less amount of Brønsted acid centers, they transform glycerol more efficiently. The higher surface area of the sulfonated OMC catalyst should favor a better distribution of the acid centers and, therefore, the accessibility of the reagents to the acid sites.

In order to increase the conversion and selectivity to h-GTBE of catalyst S24–*C*-Xyl-E2, another catalytic test was carried out at a longer reaction time to favor the evolution of the consecutive reactions, and using the catalyst previously dried, since we observed by TGA high water content for sulfonated OMCs. If the acid sites are surrounded by a hydrated layer, they could lose their strength. Therefore, to avoid the presence of water during the reaction, catalyst S24–*C*-Xyl-E2 was transferred directly out of the drying furnace at 80 °C into the reaction vessel (marked as * on Fig. 10). This catalyst presented after 48 h of reaction with high conversion (72%), higher TOF value, and high selectivity to di- and tri-ethers (h-GTBE) (92%) with a selectivity to the tri-ether of 32 %. Additionally, a good reproducibility of the catalytic tests was observed for this catalyst (Fig. 10). This preliminary result is comparable to the best results published in the literature using sulfonated SBA-15 and sulfonated beta zeolite catalysts, which achieved total conversion and high selectivity (up to 91 %) towards h-GTBE at 75 °C [14]. This proves the potentiality of this OMC-based catalyst for Brønsted acid-catalyzed reactions.

Fig. 11 shows the proposed mechanism for the etherification of glycerol with isobutene on sulfonated OMCs catalyst based on previous reported studies using other Brønsted acid catalysts [42]. Isobutene, in

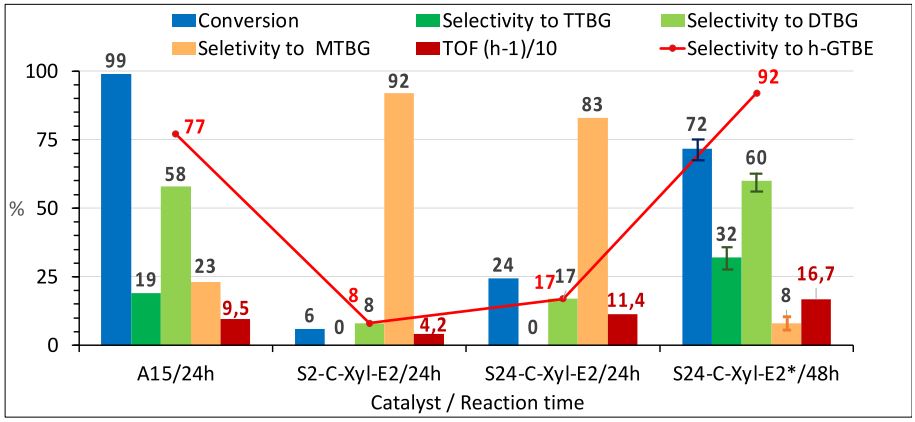

Fig. 10. Catalytic Activity of acid-sulfonic ordered mesoporous carbons obtained from xylose extract for the glycerol etherification reaction. Reaction conditions: 80 °C, reaction time 24 h or 48 h, Ratio Glycerol/Isobutene 1:4, 5 wt % of catalyst. MTBG: glycerol monoethers; DTBG: glycerol diethers; TTBG: glycerol triether; h-GTBE: glycerol diethers + glycerol triether. * catalyst dried. Error bars indicated for the best catalyst.

the presence of the Brønsted acid centers of the catalyst, led to the formation of a carbocation intermediate, which could react with either the primary or secondary hydroxyl group of glycerol to form 1-*tert*-butoxypropane-2,3-diol or 2-*tert*-butoxypropane-1,3-diol, respectively (MTBG) [42]. The subsequent consecutive formation of diethers (DTBG) and triether (TTBG) follow a similar mechanism [42].

3.5.2. Catalytic obtention of levulinic acid from 5-HMF using sulfonated OMC obtained from glucose extract

Levulinic acid (LeA) can be obtained by the catalytic transformation of 5-HMF using Brønsted acid centers [24]. Fig. 12 shows the catalytic activity results obtained using the sulfonated well-ordered carbon prepared from glucose extract (S24–*C*-Glu-E2) for the transformation of 5-HMF to levulinic acid under different reaction conditions. Commercial sulfonic macroporous resin Amberlyst (A15) was also tested for comparison. Different temperatures and the use of γ-valerolactone (GVL) as a co-solvent were studied.

All catalysts were active for the obtention of levulinic acid. No other reaction products were detected by gas chromatography. The other reaction products should be oligomers formed by the etherification of two molecules of 5-HMF or by esterification of 5-HMF with LeA, as previously described in the literature for this reaction [24].

Catalyst S24–*C*-Glu-E2, obtained after impregnation of *C*-Glu-E2 with H_2SO_4 at 80 °C for 24 h, exhibited high conversion (75 %) and moderate selectivity to LeA (33 %) at 180 °C after 1.15 h using water as solvent. Interestingly, this sulfonated OMC catalyst had almost 6 times higher TOF value than the Amberlyst-15 catalyst tested at the same reaction conditions (Fig. 12), although having less amount of Brønsted acid centers (Table 4). This behavior was similar to that previously observed for the etherification of glycerol to obtain h-GTBE and can be related to the better distribution and accessibility of the Brønsted acid centers due to the higher surface area of the sulfonated OMC catalyst.

A decrease in the reaction temperature and the use of GVL as a co-solvent led to a decrease in conversion and TOF values but resulted in an increase in the selectivity to LeA for both catalysts. Under these reaction conditions, catalyst S24–*C*-Glu-E2 achieved a selectivity to LeA up to 39 %. These results did not improve those previously published using ionic liquid functionalized mesoporous organosilica nanospheres for this reaction [24]. However, good reproducibility of the catalytic tests was observed for this catalyst (Fig. 12). This reaction requires higher control of acidity, as the strong Brønsted acid sulfonic groups present in the sulfonated OMC favor the undesired secondary polymerization reactions.

Fig. 13 shows the proposed mechanism for the conversion of 5-hydroxymethylfurfural to levulinic acid on acid-functionalized OMC catalysts considering those previously published using other Brønsted acid catalysts for this reaction [43,44]. Hydration of 5-HMF consists of the addition of a water molecule to the C2–C3 olefinic bond of the furan ring, leading to an unstable tricarbonyl intermediate, which quickly evolves to levulinic acid and formic acid (HCOOH) in the presence of Brønsted acid sites [43,44].

3.5.3. Catalytic hydrodeoxygenation of guaiacol using OMCs obtained from lignin extract as catalytic supports or bifunctional catalysts

Hydrodeoxygenation of guaiacol is a very complex reaction in which hydrogenation, demethoxylation, deoxygenation and dehydration processes are involved (Scheme 1c). Ni catalyst supported on OMC obtained from lignin (Ni/C-Lig-E2) led to total conversion, 58 % of selectivity to methoxycyclohexanol, which was the main product, and 13 % of selectivity to cyclohexanol (Fig. 14). Cyclohexane was not detected for this catalyst. This result indicates that the catalyst had high hydrogenating ability since the reaction products were fully hydrogenated molecules. However, deoxygenation was not totally achieved. This catalytic result agrees with the results obtained by other supported nickel catalysts for this reaction [25,27,45] especially at reaction temperatures below 200 °C [26,46].

Several authors reported that the guaiacol HDO activity of supported metal catalysts can be improved by incorporating additional Brønsted acid sites, usually H-zeolites, through a synergetic effect between metallic and acid sites [26,46–48]. Thus, several catalysts were prepared by mixing physically 100 mg of Ni/C-Lig-E2 and 100 mg of H-Beta (579 m^2/g, 0.60 mmol H^+/g), 100 mg of S2–*C*-Lig-E2, 300 mg of S2–*C*-Lig-E2 or 100 mg of S24–*C*-Lig-E2 to be tested for this reaction (Fig. 14).

The addition of 100 mg of sulfonated OMCs obtained from lignin (S2–*C*-Lig-E2 and S24–*C*-Lig-E2) allowed us to detect cyclohexane in low amounts (1–3 %), the selectivity to cyclohexanol was maintained (13–14 %), and the main product was again methoxycyclohexanol, which was obtained in higher amounts (65–77 %) at expenses of the other reaction products for a total conversion. The small differences between both catalysts can be related to the similar acidity of the sulfonated OMCs used (Table 4).

When combining 100 mg of H-beta zeolite with 100 mg of Ni/C-Lig-E2, 78 % of selectivity for cyclohexane was obtained for a total conversion. This means that H-beta has the appropriate amount and strength of acid centers to favor the HDO of guaiacol. Additionally, these catalytic results were reproducible for this catalyst (Fig. 14).

In order to increase the amount of acid centers and try to improve the selectivity to cyclohexane using sulfonic-acid OMCs, one more catalyst was prepared by combining 100 mg of *C*-Lig-E2 with 300 mg of S2–*C*-Lig-E2. Although the selectivity to cyclohexane increased up to 5 %, the formation of other reaction products increased spectacularly. Among these other products, we identified cyclohexene and cyclohexanone, which were not observed for the rest of the catalysts. The stronger Brønsted acid sites of sulfonated OMCs compared to H-Beta together with the possible covering of metallic sites by the acidic ones, could explain this catalytic behavior.

Finally, 100 mg of Ni/C-Lig-E6, prepared using a more crystalline OMC and with 10 % more reduced metallic Ni with respect to Ni/C-Lig-E2, was combined with 100 mg of H-Beta to check its catalytic behavior. 60 % of selectivity to cyclohexane was obtained for a 93 % conversion (Fig. 14), being therefore, similar to the catalytic behavior of the mixture prepared with Ni/C-Lig-E2. This can be explained by the low differences observed from the characterization of these two Ni/OMC catalysts.

Fig. 15 shows the proposed mechanism for the hydrodeoxygenation of guaiacol to cyclohexane at low temperatures on Ni/OMC catalyst combined with H-Beta following the mechanism proposed by Wang

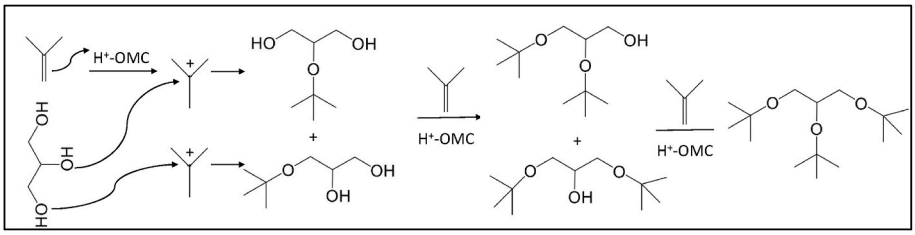

Fig. 11. Proposed mechanism for the etherification of glycerol with isobutene on sulfonated ordered mesoporous carbons.

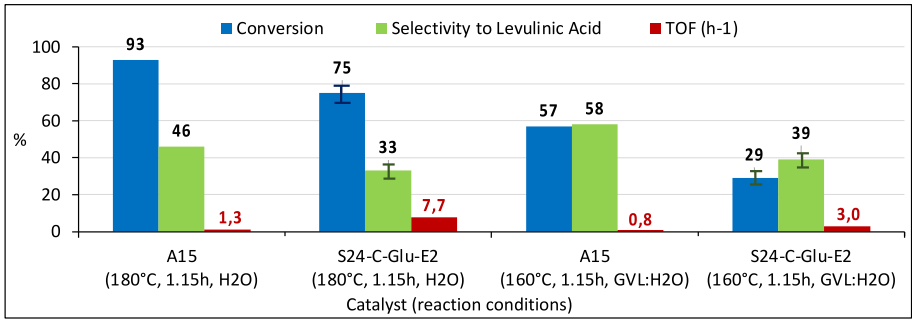

Fig. 12. Catalytic activity of sulfonated ordered mesoporous carbon obtained from glucose extract, sulfonated SBA-15 and Amberlyst-15 for the conversion of 5-hydroxymethylfurfural to levulinic acid at different reaction conditions and solvents. GVL: γ-valerolactone. Error bars indicated for the best catalysts.

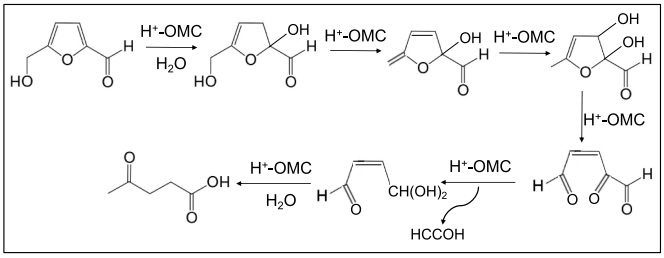

Fig. 13. Proposed mechanism for the conversion of 5-hydroxymethylfurfural to levulinic acid on sulfonated ordered mesoporous carbons.

et al. [26]. The first step consists of the hydrogenation of the aromatic ring on the Ni metallic centers to form 2-methoxycyclohexanol, which is then demethoxylated-dehydrated on the Brønsted acid sites of the H-beta zeolite forming cyclohexenol, which is readily hydrogenated by the Ni metallic centers to cyclohexanol. In the presence of Brønsted acid sites, cyclohexanol can be dehydrated to cyclohexene, which can be easily hydrogenated by the Ni metallic centers to cyclohexane.

Anyway, using an OMC obtained from lignin combined with H-Beta, high selectivity to cyclohexane for a total conversion was obtained. This catalytic result is comparable to those previously published for this reaction using Ni/SiO_2 + H-Beta mixtures [26] and shows the potential of using OMC derived from biomass as catalytic support of metal catalysts.

4. Conclusions

Well-ordered OMCs with high surface areas (576–948 m^2/g) were successfully synthesized from xylose, glucose and lignin solutions obtained from almond shells. Acidic medium favored polymerization-carbonization reaction when using glucose or xylose. Ultrasounds facilitated the diffusion of the carbon precursors inside the mesopores of the template. The concentration of the lignin extract influenced the crystallinity of the OMC. The appropriate carbon precursor/template ratio and the optimized carbonization temperature were different for each biomass extract. The preliminary catalytic results obtained with these OMCs, used as catalysts or as catalytic supports for three reactions of interest, showed the high potentiality of these materials in the field of catalysis.

Full conversion and 92% selectivity to di- and tri-ethers of glycerol were obtained using a dried sulfonic-acid treated OMC catalyst, obtained from xylose extract, for the glycerol etherification. A higher turnover frequency value and slightly lower selectivity to levulinic acid than commercial Amberlyst-15 were achieved using a sulfonic-acid treated OMC, obtained from glucose, for the conversion of 5-hydroxymethylfurfural. Total conversion and 78 % of selectivity to cyclohexane were obtained using an OMC obtained from lignin as catalytic support of a nickel catalyst combined with H-Beta for the hydrodeoxygenation of guaiacol.

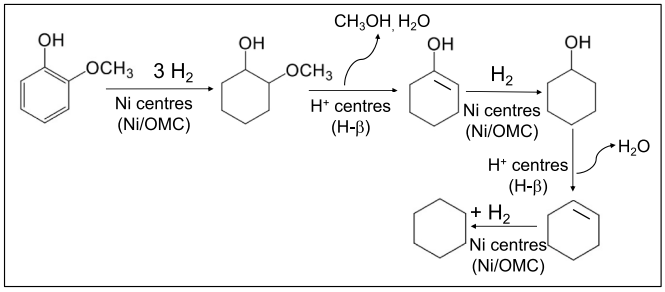

Fig. 15. Proposed mechanism for the hydrodeoxygenation of guaiacol to cyclohexane on Ni/OMC catalyst combined with H-Beta at low reaction temperatures.

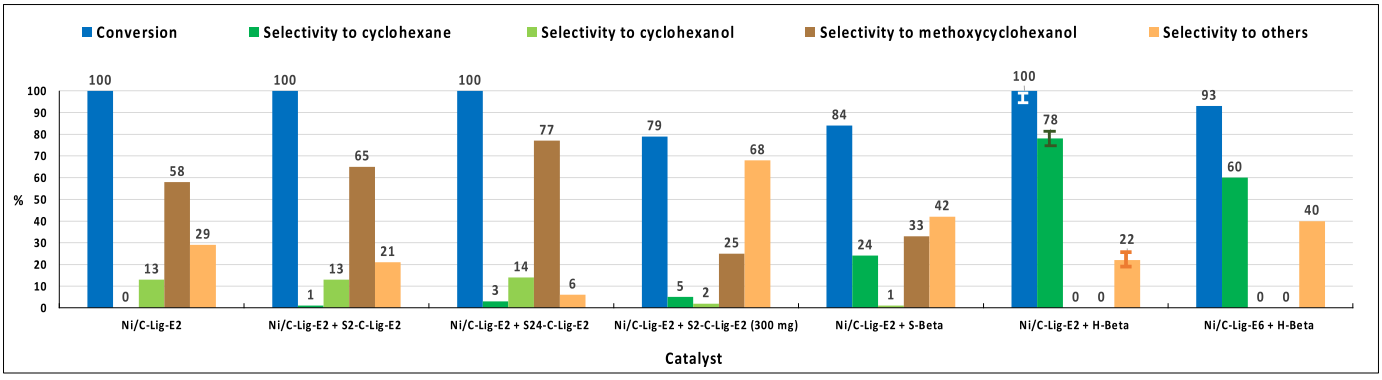

Fig. 14. Catalytic activity of Ni/OMC catalysts for the hydrodeoxygenation of guaiacol. Reaction conditions: 200 mg of guaiacol, 180 °C, 30 bars H_2, 1 h. Error bars indicated for the best catalyst.

CRediT authorship contribution statement

Anna Casadó: Visualization, Validation, Investigation. **Anies Rösch:** Visualization, Validation, Investigation. **Angie C. Rueda:** Visualization, Validation, Investigation. **Alejandro Uribe:** Visualization, Validation, Investigation. **M. Dolores González:** Writing – original draft, Supervision, Conceptualization. **Aroldo J. Romero:** Validation, Supervision, Investigation, Conceptualization. **Joan J. Carvajal:** Supervision, Conceptualization. **Yolanda Cesteros:** Writing – review & editing, Writing – original draft, Supervision, Resources, Funding acquisition, Conceptualization.

Declaration of competing interest

The authors declare that they have no known competing financial interests or personal relationships that could have appeared to influence the work reported in this paper.

Data availability

The data that has been used is confidential.

Acknowledgements

This work was supported by the project PID2019-110735RB-C22 funded by MICIU/AEI/10.13039/501100011033, and by the projects 2021/19 and 2022/20 funded by Diputació de Tarragona. Dr. A. J. Romero-Anaya thanks European Union's Horizon 2020 research and innovation programme under Marie Sklodowska Curie grant agreement No712949 and Generalitat de Catalunya (TECNIOspring project TECSPR18-1-0051), for the financial support provided during years 2019–2021. A. Casadó and A.C. Rueda thank Generalitat de Catalunya for the FISDUR grant 2021 (Ref. FISDUR 00181) and FI grant 2022 (Ref. FI_B 00128), respectively. We acknowledge Jordi Sanahujes de Barrena Sarobe for his help in the obtention of the biomass fractions used for this project.

References

[1] M. Enterría, J.L. Figueiredo, Nanostructured mesoporous carbons: tuning texture and surface chemistry, Carbon 108 (2016) 79–102, https://doi.org/10.1016/j.carbon.2016.06.108.

[2] Z.E. Tang, S. Lim, Y.L. Pang, H.C. Ong, K.T. Lee, Synthesis of biomass as heterogeneous catalyst for application in biodiesel production: state of the art and fundamental review, Renew. Sustain. Energy Rev. 92 (2018) 235–253, https://doi.org/10.1016/j.rser.2018.04.056.

[3] S. Jun, S.H. Joo, R. Ryoo, M. Kruk, M. Jaroniec, Z. Liu, T. Ohsuna, O. Terasaki, Synthesis of new, nanoporous carbon with hexagonally ordered mesostructure, J. Am. Chem. Soc. 122 (2000) 10712–10713, https://doi.org/10.1021/ja002261e.

[4] Y. Xia, Z. Yang, R. Mokaya, Templated nanoscale porous carbons, Nanoscale 2 (2010) 639–659, https://doi.org/10.1039/B9NR00207C.

[5] H. Nishihara, T. Kyotani, Templated nanocarbons for energy storage, Adv. Mater. 24 (2012) 4473–4498, https://doi.org/10.1002/adma.201201715.

[6] M.R. Benzigar, S. Joseph, H. Ilbeygi D.-H. Park, S. Sarkar, G. Chandra, S. Umapathy, S. Srinivasan, S.N. Talapaneni, A. Vinu, Highly crystalline mesoporous C60 with ordered pores: a class of nanomaterials for energy applications, Angew. Chem. Int. Ed. 57 (2018) 569–573, https://doi.org/10.1002/anie.201710888.

[7] Z. Wang, W. Han, H. Tang, Y. Li, H. Liu, Preparation of N-doped ordered mesoporous carbon and catalytic performance for the pyrolysis of 1-chloro-1,1-difluoroethane to vinylidene fluoride, Microporous Mesoporous Mater. 275 (2019) 200–206, https://doi.org/10.1016/j.micromeso.2018.08.020.

[8] M. Inagaki, M. Toyoda, Y. Soneda, S. Tsujimura, T. Morishita, Templated mesoporous carbons: synthesis and applications, Carbon 107 (2016) 448–473, https://doi.org/10.1016/j.carbon.2016.06.003.

[9] R. Liu, X. Wang, X. Zhao, P. Feng, Sulfonated ordered mesoporous carbon for catalytic preparation of biodiesel, Carbon 46 (2008) 1664–1669, https://doi.org/10.1016/j.carbon.2008.07.016.

[10] W. Xin, Y. Song, Mesoporous carbons: recent advances in synthesis and typical applications, RSC Adv. 5 (2015) 83239–83285, https://doi.org/10.1039/C5RA16864C.

[11] Y.N. Liang, W. Oh, Y. Li, X. Hu, Nanocarbons as platforms for developing novel catalytic composites: overview and prospects, Appl. Catal. Gen. 562 (2018) 94–105, https://doi.org/10.1016/j.apcata.2018.05.021.

[12] E. Doustkhah, J. Lin, S. Rostamnia, C. Len, R. Luque, X. Luo, Y. Bando, K.C.-W. Wu, J. Kim, Y. Yamauchi, Y. Ide, Development of sulfonic-acid-functionalized mesoporous materials: synthesis and catalytic applications, Chem. Eur J. 25 (2019) 1614–1635, https://doi.org/10.1002/chem.201802183.

[13] X. Wang, M. Qiu, Y. Tang, J. Yang, F. Shen, X. Qi, Y. Yu, Synthesis of sulfonated lignin-derived ordered mesoporous carbon for catalytic production of furfural from xylose, Int. J. Biol. Macromol. 187 (2021) 232–239, https://doi.org/10.1016/j.ijbiomac.2021.07.155.

[14] M.D. González, Y. Cesteros, J. Llorca, P. Salagre, Boosted selectivity toward high glycerol tertiary butyl ethers by microwave-assisted sulfonic acid-functionalization of SBA-15 and beta zeolite, J. Catal. 290 (2012) 202–209, https://doi.org/10.1016/j.jcat.2012.03.019.

[15] M.D. González, P. Salagre, E. Taboada, L. Llorca, Y. Cesteros, Microwave-assisted synthesis of sulfonic acid-functionalized microporous materials for the catalytic etherification of glycerol with isobutene, Green Chem. 15 (8) (2013) 2230–2239, https://doi.org/10.1039/C3GC40683K.

[16] M.D. González, P. Salagre, E. Taboada, J. Llorca, E. Molins, Y. Cesteros, Sulfonic acid-functionalized aerogels as high resistant to deactivation catalysts for the etherification of glycerol with isobutene, Appl. Catal. B Environ. 136–137 (2013) 287–293, https://doi.org/10.1016/j.apcatb.2013.02.018.

[17] M.D. González, P. Salagre, R. Mokaya, Y. Cesteros, Tuning the acidic and textural properties of ordered mesoporous silicas for their application as catalysts in the etherification of glycerol with isobutene, Catal. Today 227 (2014) 171–178, https://doi.org/10.1016/j.cattod.2013.10.029.

[18] M. Goncalves, C. Castro, L. Oliveira, W. Carvalho, Green acid catalyst obtained from industrial wastes for glycerol etherification, Fuel Process. Technol. 138 (2015) 695–703, https://doi.org/10.1016/j.fuproc.2015.07.010.

[19] L. Frusteri, C. Cannilla, G. Bonura, A. Chuvilin, S. Perathoner, G. Centi, F. Frusteri, Carbon microspheres preparation, graphitization and surface functionalization for glycerol etherification, Catal. Today 277 (2016) 68–77, https://doi.org/10.1016/j.cattod.2016.02.044.

[20] R. Estevez, L. Aguado-Deblas, V. Montes, A. Caballero, F.M. Bautista, Sulfonated carbons from olive stones as catalysts in the microwave-assisted etherification of glycerol with tert-butyl alcohol, Mol. Catal. 488 (2020) 110921, https://doi.org/10.1016/j.mcat.2020.110921.

[21] X. Li, R. Xu, J. Yang, S. Nie, D. Liu, Y. Liu, C. Si, Production of 5-hydroxymethylfurfural and levulinic acid from lignocellulosic biomass and catalytic upgradation, Ind. Crops Prod. 130 (2019) 184–197, https://doi.org/10.1016/j.indcrop.2018.12.082.

[22] X. Cheng, Q. Feng, D. Ma, H. Chen, X. Zeng, F. Xing, J. Teng, Eco-Friendly synthesis of SO_3H-containing solid acid via mechanochemistry for the conversion of carbohydrates to 5-hydroxymethylfurfural, J. Environ. Chem. Eng. 9 (2021) 105747, https://doi.org/10.1021/acssuschemeng.0c00784.

[23] Z. Chen, S. Zhang, B. Yan, Q. Cai, S. Zhang, Lignin-based solid acid catalyst for cellulose residue conversion into levulinic acid in biphasic system, Ind. Crops Prod. 178 (2022) 114523, https://doi.org/10.1016/j.indcrop.2022.114523.

[24] D. Song, J. Liu, C. Zhang, Y. Guo, Design of Brønsted acidic ionic liquid functionalized mesoporous organosilica nanospheres for efficient synthesis of ethyl levulinate and levulinic acid from 5-hydroxymethylfurfural, Catal. Sci. Technol. 11 (2021) 1827–1842, https://doi.org/10.1039/D0CY01941K.

[25] A.B. Dongil, I.T. Ghampson, R. García, J.L.G. Fierro, N. Escalona, Hydrodeoxygenation of guaiacol over Ni/carbon catalysts: effect of the support and Ni loading, RSC Adv. 6 (2016) 2611–2623, https://doi.org/10.1039/C5RA22540J.

[26] X. Wang, S. Zhu, S. Wang, Y. He, Y. Liu, J. Wang, W. Fan, Y. Lv, Low temperature hydrodeoxygenation of guaiacol into cyclohexane over Ni/SiO_2 catalyst combined with Hβ zeolite, RSC Adv. 9 (2019) 3868–3876, https://doi.org/10.1039/C8RA09972C.

[27] M. López, R. Palacio, S. Royer, A.-S. Mamede, J.J. Fernández, Mesostructured CMK-3 carbon supported Ni–ZrO_2 as catalysts for the hydrodeoxygenation of guaiacol, Microporous Mesoporous Mater. 292 (2020) 109694, https://doi.org/10.1016/j.micromeso.2019.109694.

[28] V. Sánchez, A. Dafinov, P. Salagre, J. Llorca, Y. Cesteros, Microwave-Assisted furfural production using hectorites and fluorohectorites as catalysts, Catalysts 9 (2019) 706, https://doi.org/10.3390/catal9090706.

[29] K.J. Kowalski, J. Król, P. Radziszewski, R. Casado, V. Blanco, D. Pérez, V.M. Viñas, Y. Brijsse, M. Frosch, D.M. Le, M. Wayman, Eco-friendly materials for a new concept of asphalt pavement, Transport. Res. Procedia 14 (2016) 3582–3591, https://doi.org/10.1016/j.trpro.2016.05.426.

[30] C. N Hamelinck, G. van Hooijdonk, A.P.C. Faaij, Ethanol from lignocellulosic biomass: techno-economic performance in short-, middle- and long-term, Biomass Bioenergy 28 (2005) 384–410, https://doi.org/10.1016/j.biombioe.2004.09.002.

[31] R.J. Hill, C.J. Howard, Quantitative phase analysis from neutron powder diffraction data using the Rietveld method, J. Appl. Crystallogr. 20 (1987) 467–474, https://doi.org/10.1107/S0021889887086199.

[32] D. Balzar, Voigt-function model in diffraction line-broadening analysis, in: R. L. Snyder, J. Fiala, H.J. Bunge (Eds.), Defect and Microstructure Analysis by Diffraction (International Union of Crystallography Monographs on Crystal), Oxford University Press, Oxford, 1999, pp. 94–124.

[33] H.K.D. Nguyen, H.Q. Tran, Thermal stability of ordered mesoporous carbon based catalyst and its application in conversion of linseed oil to methyl esters, Catal. Lett. 150 (2020) 1028–1040, https://doi.org/10.1007/s10562-019-03001-4.

[34] J.A. Melero, G.D. Stucky, R. van Grieken, G. Morales, Direct syntheses of ordered SBA-15 mesoporous materials containing arenesulfonic acid groups, J. Mater. Chem. 12 (2002) 1664–1670, https://doi.org/10.1039/B110598C.

[35] J. Schönherr, J.R. Buccheim, P. Scholz, P. Adelhelm, Titration Revisited (Part I): Practical Aspects for Achieving a high Precision in Quantifying Oxygen-Containing

Surface Groups on Carbon Materials 4 (2) (2018) 21, https://doi.org/10.3390/c4020021. C.
[36] M.E. Jamróz, M. Jarosz, J. Witowska-Jarosz, E. Bednarek, W. Teeza, M.H. Jamróz, J.C. Dobrowolski, J. Kijenski, Mono-, di-, and tri-tert-butyl ethers of glycerol: a molecular spectroscopic study, Spectrochim. Acta Mol. Biomol. Spectrosc. 67 (2007) 980, https://doi.org/10.1016/j.saa.2006.09.017.
[37] S. Herou, M.C. Ribadeneyra, R. Madhu, V. Araullo-Peters, A. Jensen, P. Schlee, M. Titirici, Ordered mesoporous carbons from lignin: a new class of biobased electrodes for supercapacitors, Green Chem. 21 (2019) 550–559, https://doi.org/10.1039/C8GC03497D.
[38] L. Gan, L. Lyu, T. Shen, S. Wang, Sulfonated lignin-derived ordered mesoporous carbon with highly selective and recyclable catalysis for the conversion of fructose into 5-hydroxymethylfurfural, Appl. Catal., A 574 (2019) 132–143, https://doi.org/10.1016/j.apcata.2019.02.008.
[39] X. Wang, X. Liu Jr., R.L. Smith, Y. Liang, X. Qi, Direct one-pot synthesis of ordered mesoporous carbons from lignin with metal coordinated self-assembly, Green Chem. 23 (2021) 8632–8642, https://doi.org/10.1039/D1GC03030B.
[40] Y. Liang, X. Liu, X. Qi, Hierarchical nanoarchitectonics of ordered mesoporous carbon from lignin for high-performance supercapacitors, Int. J. Biol. Macromol. 213 (2022) 610–620, https://doi.org/10.1016/j.ijbiomac.2022.06.005.
[41] R.P. Rocha, M.F.R. Pereira, J.L. Figuereido, Characterization of the surface chemistry of carbon materials by temperature-programmed desorption: an assessment, Catal. Today 418 (2023) 114136, https://doi.org/10.1016/j.cattod.2023.114136.
[42] P. Palanychamy, S. Lim, Y.H. Yap, L.K. Leong, Critical review of the various reaction mechanisms for glycerol etherification, Catalysts 12 (2022) 1487, https://doi.org/10.3390/catal12111487.
[43] S. Kanga, J. Fub, G. Zhanga, From lignocellulosic biomass to levulinic acid: a review on acid-catalyzed hydrolysis, Renew. Sustain. Energy Rev. 94 (2018) 340, https://doi.org/10.1016/j.rser.2018.06.016.
[44] C. Antonetti, D. Licursi, S. Fulignati, G. Valentini, A.M. Raspolli Galletti, New frontiers in the catalytic synthesis of levulinic acid: from sugars to raw and waste biomass as starting feedstock, Catalysts 6 (2016) 196, https://doi.org/10.3390/catal6120196.
[45] A.B. Dongil, L. Pastor-Pérez, A. Sepúlveda-Escribano, R. García, N. Escalona, Hydrodeoxygenation of guaiacol: tuning the selectivity to cyclohexene by introducing Ni nanoparticles inside carbon nanotubes, Fuel 172 (2016) 65–69, https://doi.org/10.1016/j.fuel.2016.01.002.
[46] S. Qiu, Y. Xu, Y. Weng, L. Ma, T. Wang, Efficient hydrogenolysis of guaiacol over highly dispersed Ni/MCM-41 catalyst combined with HZSM-5, Catalysts 6 (2016) 134, https://doi.org/10.3390/catal6090134.
[47] M. Hellinger, H.W.P. Carvalho, S. Baier, D. Wang, W. Kleist, J.D. Grunwaldt, Hydrodeoxygenation of guaiacol as a model compound of bio-oil in methanol over mesoporous noble metal catalysts, Appl. Catal., A 490 (2015) 181–192, https://doi.org/10.1016/j.apcata.2018.01.008.
[48] W.J. Song, Y.S. Liu, E. Barath, C. Zhao, J.A. Lercher, Synergistic effects of Ni and acid sites for hydrogenation and C–O bond cleavage of substituted phenols, Green Chem. 17 (2015) 1204–1218, https://doi.org/10.1039/C4GC01798F.